Heat Transfer in the Critical Region

R. P. BRINGER and J. M. SMITH

Purdue University, Lafayette, Indiana

Heat transfer coefficients were measured experimentally for carbon dioxide in turbulent flow in an 0.18-in. I.D. pipe. The pressure was 1,200 lb./sq. in. abs. and the bulk temperature varied from 70° to 120°F. In this critical region the coefficients between fluid and tube wall ranged from 300 to 2,600 B.t.u./(hr.)(sq. ft./°F.) over a Reynolds number interval of 30,000 to 300,000.

Existing empirical and semitheoretical correlations were found inadequate in this region, where the thermal conductivity, viscosity, density, and specific heat are all varying rapidly and nonuniformly with temperature. A method of integrating the heat and momentum transfer equations with variable physical properties, recently proposed by Deissler, was applied to the experimental data and found to fit well. The application required extensive calculations, which were carried out with an Electrodata digital computer.

A simplified procedure was proposed for estimating heat transfer coefficients in the critical region by using a semitheoretical equation developed for zero heat flow. Simple rules were suggested for estimating the temperature at which to evaluate the physical properties when this equation is applied to the real case of finite heat transfer. The method worked well when compared with the computed heat transfer coefficients of Deissler for supercritical water but showed about 30% deviation when compared with the carbon dioxide results. This discrepancy is believed due to the fact that the carbon dioxide was very close to the critical point (reduced pressure = 1.1) but the water was somewhat further removed (reduced pressure = 1.6).

Empirical correlations of heat transfer coefficients for fluids flowing in circular tubes have been available for many years (*9, 20, 21*), and semitheoretical methods based upon relating the transfer of momentum and heat have also been developed (*1, 27*). Both procedures give dependable results when the physical properties of the fluid do not vary greatly from the center of the conduit to the tube wall. This condition prevails when the temperature change across the tube diameter is negligible, and hence the correlations often have been described as applying at isothermal conditions. Perhaps the first practical problem in which deviations from this condition were severe was in the heating or cooling of viscous petroleum fractions, where the viscosity change across the tube was large and the conventional correlations did not apply. An empirical modification, using the ratio $(\mu_0/\mu_b)^a$, was successfully introduced by Sieder and Tate (*24*) to handle this case.

With the development of gas turbines, rocket motors, and high-pressure steam power plants, the problem of variable physical properties has become much more severe. Large temperature differences between the fluid and the tube wall at ordinary pressure can cause severalfold changes in the thermal conductivity, viscosity, and specific heat (except for diatomic gases); however, as long as the critical pressure is not approached the variations are uniform and exhibit no unusual characteristics. The most severe case is encountered when the fluid is in the critical region, for here the changes in properties are both irregular and large for small variations in temperature.

The purpose of this investigation was to measure heat transfer coefficients in the critical region and to develop a method of correlating the results so that predictions might be made without heat transfer measurements. Carbon dioxide was chosen as the fluid because of its intermediate critical temperature and because its physical and thermal properties are fairly well established.

EXPERIMENTAL METHOD

The experimental method consisted of measuring the energy transferred to carbon dioxide flowing through a tube. The large variation in physical properties combined with entrance effects makes it impossible to maintain a constant heat transfer coefficient along a finite length of tube. Hence measurements taken over a section of tube would lead to average values of h which would have little significance. It was accordingly necessary to determine a local or point heat transfer coefficient defined by the expression

$$q_0 = h(t_0 - t_b) \qquad (1)$$

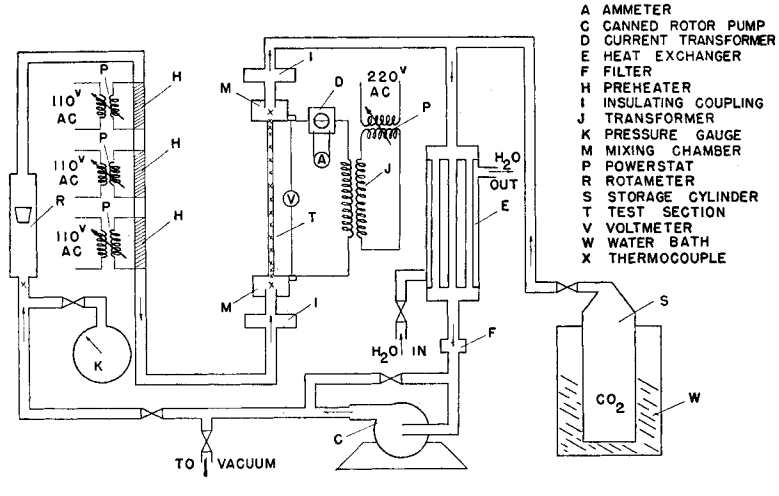

Fig. 1. Experimental apparatus.

R. P. Bringer is at present with Dow Chemical Company, Midland, Michigan, and J. M. Smith is at the University of New Hampshire, Durham, New Hampshire.

where q_0 is the local rate of heat transfer per unit area at the wall and t_0 and t_b are the wall and bulk fluid temperatures. The measurement of the heat transfer rate at any point is facilitated by electrical heating, with the current passed directly through the tube wall. If, in addition, a material is used which has an electrical resistivity independent of temperature, q_0 for a given voltage becomes the same at any point along the tube. This is important because it means that the variations in wall temperature along the tube length will be reduced and be caused by only the change in fluid temperature and heat transfer coefficient. With a variable electrical resistivity q_0 becomes a function of wall temperature and the interpretation of the results is more difficult.

The bulk fluid temperature was determined by the following heat balance

$$I^2R_t\left(\frac{z}{L}\right) = w(H_b - H_1) \qquad (2)$$

where H_b represents the enthalpy of the carbon dioxide at the bulk-mean temperature at the point z distance from the entrance to the test section of the tube. The temperature t_b can be found after H_b is determined from Equation (2) by reference to the thermodynamics properties of carbon dioxide.

The wall temperature was measured directly by thermocouples attached to the tube wall as described in the next section.

APPARATUS

The complete equipment, illustrated in Figure 1, consists of a closed circuit in which carbon dioxide is heated in the test section T and cooled in the heat exchanger E. The canned-rotor pump C was constructed according to the design developed by the Oak Ridge National Laboratory for a high-suction-pressure, high-temperature, totally enclosed unit (*28*). The pump was made from type 300 stainless steel materials, except for the bearings of Graphitar No. 14 and the chrome plate in the journal of the rotor. The unit was entirely satisfactory for the service required in this study.

The test section consisted of an Inconel tube 0.25 in. O.D., 0.035 in. of wall thickness and 24.0 in. long. The high tensile strength of Inconel made it possible to use a thin-walled tube and thus to obtain the desired heat input. Also the temperature coefficient of electrical resistivity (0.00069 ohm ft./°F.) was sufficiently low that temperature variations along the tube had no appreciable effect on its resistance. Identical mixing chambers were silver soldered to each end of the Inconel tube. The chambers were fashioned from 2-in.-diam. steel stock bored with a circular hole 1 in. in diameter. The details of a chamber fitted with thermocouple and shield are shown in Figure 2. The shield provided an adiabatic section for temperature measurement in addition to providing for mixing of the fluid. The thermocouples were made from 30-gauge copper-constantan wire and inserted into the center of the mixing space, thus providing a ½-in. isothermal length before the metal wall was reached. Electrical insulation was provided by insulating couplings made by inserting sheets of mica between stainless steel flanges as shown in Figure 3, where the complete test section is illustrated.

Outer surface temperatures of the tube wall were measured with fifteen copper-constantan glass-insulated thermocouples located at 0, 1, 2, 4, 6, 8, 10, 12, 14, 16, 18, 20, 22, 23, and 24 in. from the tube entrance, as indicated in Figure 3. The couples were spot-welded to the tube wall and then the lead wires wound around the tube for several turns before leaving the test section through the Fiberglas insulation (2 in. thick). The measured values were corrected to inside surface temperatures (commonly referred to as *wall* temperatures) by use of the known heat flux, tube thickness, and diameter, and thermal conductivity of Inconel as a function of temperature.

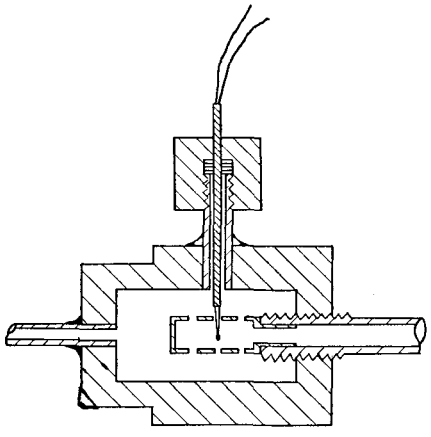

Fig. 2. Mixing chamber.

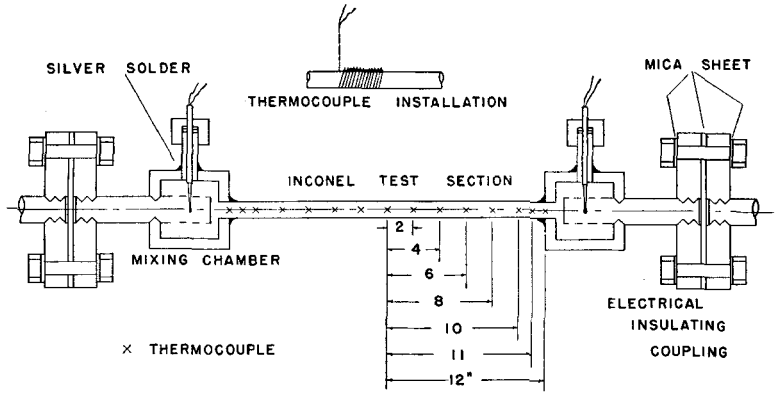

Fig. 3. Assembled test section.

SCOPE OF INVESTIGATION

In order to simplify the comparison of the experimental results for the heat transfer coefficient with theoretical predictions, it was desirable to operate the test section at essentially constant pressure and constant wall temperature. The wall temperature does not remain constant along the entire length of tube (see Figure 8). However it was possible to obtain h at a constant wall temperature since the coefficient could be computed at any point along the tube. All that was necessary was to calculate h at a location where the inside-wall temperature was equal to the desired value. Unless this point occurred in the central 10 in., where entrance and exit effects were negligible, the run was not used. This situation is illustrated in Figure 4, where the temperature profiles for run 59 are plotted. In this instance an inside-surface-wall temperature of 110°F. was required, corresponding to a measured outer surface value of 115°F. Reference to the figure (solid line) indicates that this temperature occurred a little beyond the midway point along the tube. The dotted line shows the approximate fluid temperature (bulk mean) profile.

Since the heat input per unit length was constant for the whole tube, Figure 4 can be used to illustrate how the heat transfer coefficient varies with position. At the entrance h has a very high value and then decreases as entrance thermal effects disappear. In the central section variations in h are less and are due to the effect of changes in the physical properties of carbon dioxide.

The equipment was then operated at constant heat flux, and at a pressure of 1,200 lb./sq. in. abs. (the critical value is 1,070 lb./sq. in. abs.). The heat fluxes were chosen so as to give wall temperatures, in the central portion of the test section, of 100, 110, 130, and 150°F. The heat input and entrance temperature and flow rate of

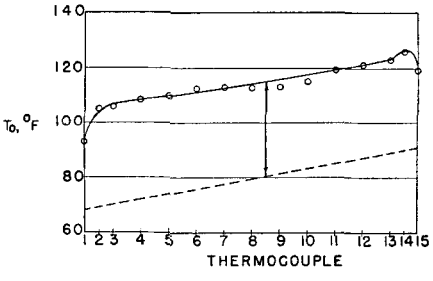

Fig. 4. Wall temperature profile for run 59.

carbon dioxide were varied to give the following range of conditions:

Reynolds number	30,000 to 300,000
Heat transfer rate, B.t.u./(hr.)(sq. ft.)	10,000 to 100,000
Carbon dioxide temperature, °F. (critical value 88°F.)	70–120

PHYSICAL PROPERTIES

In order to calculate h from Equation (1) and to obtain the values of the Prandtl, Nusselt, and Reynolds numbers for correlation purposes, one or more of the following properties of carbon dioxide are required: density, enthalpy, specific heat, viscosity, or thermal conductivity.

Michels and Michels (*15*) have very carefully determined the *P-V-T* relations in the critical region and their results were used to establish the density as a function of temperature at 1,200 lb./sq. in. abs.

The most accurate enthalpy data appear to be those calculated by Michels and DeGroot (*16*) from the *P-V-T* results previously mentioned. These results rather than the earlier work of Plank and Kuprianoff (*19*) were used here. A plot of the enthalpy data at 1,200 lb./sq. in. abs. was used in connection with the solution of Equation (1) for the heat transfer coefficient.

The viscosity of carbon dioxide at elevated pressures has been studied by Phillips (*18*), Stakelbeck (*25*), Comings and Egly (*3*), and Schroer and Becker (*22*). Also Kiyama and Makita (*12*) made measurements over a wide range of conditions, 1 to 96 atm. and 50° to 300°C. Naldrett and Maass (*17*) carried out excellent determinations in a narrow range near the critical point. Most of the data compare favorably in overlapping regions, though carried out in different types of equipment. For this work a plot of all the data except those of Schroer and Becker was used in preparing the viscosity curve at 1,200 lb./sq. in. abs. shown in Figure 5. A specific heat curve is shown on the same graph.

Much less attention has been given to the study of thermal conductivity at high pressures. The first reliable investigation reported was that of Sellschopp (*23*), who made measurements in the range of 50° to 120°F. and 700 to 1,325 lb./sq. in. abs. His results were admittedly erroneous in the critical region because of free convection, and a curve of density vs. thermal conductivity confirms this by indicating a pronounced hump near the critical point. Krausshold (*13*) has applied a correction to these data to offset the effect of convection, and the corrected data give a smooth increasing curve of conductivity vs. density as expected. Lenoir and Comings' (*14*) independent measurements are about 15% higher than those of Sellschopp but

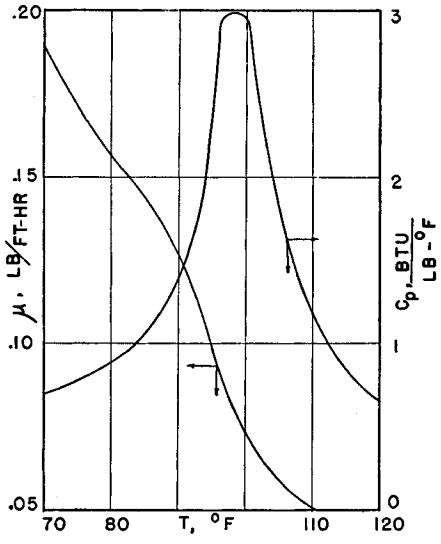

Fig. 5. Viscosity and specific heat of CO_2 at 1,200 lb./sq. in.

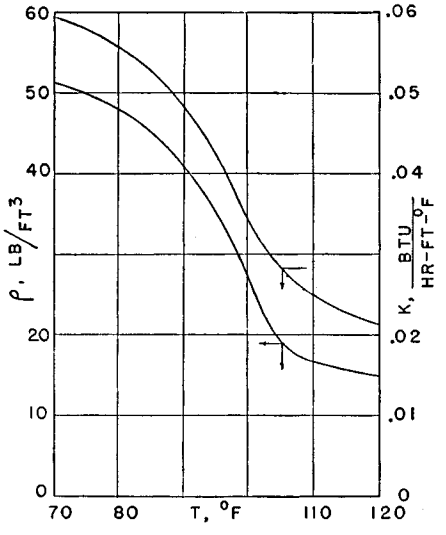

Fig. 6. Density and thermal conductivity of CO_2 at 1,200 lb./sq. in.

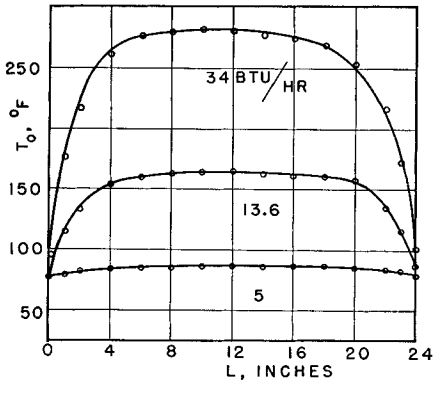

Fig. 7. Wall temperature profiles with no flow.

give a smooth k vs. p curve which parallels Krausshold's corrected curve. Franck (*11*) combined additional data by Stoljarow, et al. (*26*) with what were considered the most reliable points in the previous investigations and proposed a composite set of data. It was found that these results compared well with the values predicted by applying the law of corresponding states in the manner suggested by Lenoir and Comings (*14*). Franck's work was used in this investigation and the 1,200 lb./sq. in. abs. results are shown along with the density in Figure 6.

EXPERIMENTAL RESULTS

Equating the electrical energy input to the value of q_0 in Equation (1) is based upon the assumption of negligible heat losses radially and longitudinally from a point in the test section. To test this assumption wall-temperature profiles were measured for conditions of no flow. The results, illustrated in Figure 7, show that for a wall temperature in the central section of 150°F., the maximum employed in this study, the loss is about 12 B.t.u./hr. Since the minimum value of the total heat transferred in the runs at $t_0 = 150$°F. was 1,430 B.t.u./hr., the heat loss amounted to but 0.8%.

The flat portions of the curves in Figure 7 also show that the temperature in the central section of the tube wall is unaffected by end losses. Heat transfer coefficients for all the runs were computed from data taken in the section 7 to 17 in. from the entrance. Even at 280°F. wall temperature, far beyond the 150°F. maximum employed in the runs, the profile in the center portion is almost flat.

Analogous wall-temperature profiles with carbon dioxide flowing through the tube are shown in Figure 8 for four of the runs described in Tables 1 to 4. The central flat portions are again present. Their slope, in these cases with flow, is not zero but finite, the value depending upon the temperature rise of the carbon dioxide.

In a series of preliminary tests with water at 80° to 150°F. and low pressures, heat transfer coefficients were obtained which agreed well with the Dittus-Boelter equation. For twenty-four runs the average absolute difference between the electrical energy input to the whole test section and the heat transferred to the water, as determined by the measured inlet and outlet temperatures, was 2.4%, with twelve positive deviations and nine negative values. The maximum value was 5.0%. Water was used in these tests because its properties are well established and the heat-balance deviations would reflect the uncertainties in the equipment operation rather than in the property data.

For the carbon dioxide runs the maximum deviation was also less than 5%

TABLE 1. SAMPLE RESULTS AT t_0 = 100°F. (Pr_0 = 6.30)

Run	h, B.t.u./(hr.)(°F./sq. ft.)	Nu_0	Re_0	β	Nu_b	Re_b	Pr_b
66	650	290	50,400	0.00055	174	39,600	2.42
71	1,240	551	112,000	0.00054	328	87,000	2.37
94	825	367	49,500	0.00040	248	41,700	3.30
95	870	387	66,000	0.00044	248	55,000	2.82
99	1,625	722	145,000	0.00036	471	121,000	2.98
102	2,060	920	183,000	0.00038	595	152,000	2.97

TABLE 2. SAMPLE RESULTS AT t_0 = 110°F. (Pr_0 = 2.85)

Run	h, B.t.u./(hr.)(°F./sq. ft.)	Nu_0	Re_0	β	Nu_b	Re_b	Pr_b
46	635	382	44,000	0.0022	172	48,000	2.43
55	583	350	32,200	0.0027	157	37,000	2.44
56	1,450	873	87,500	0.0028	388	94,500	2.43
59	975	585	62,500	0.0024	266	69,000	2.54
111	2,660	1,600	155,000	0.0016	970	202,000	5.52
145	1,050	629	63,000	0.0015	382	83,000	5.64
151	2,320	1,390	158,000	0.0014	905	233,000	6.35
154	880	530	76,000	0.0007	420	97,000	5.31

TABLE 3. SAMPLE RESULTS AT t_0 = 130°F. (Pr_0 = 1.68)

Run	h, B.t.u./(hr.)(°F./sq. ft.)	Nu_0	Re_0	β	Nu_b	Re_b	Pr_b
77	620	475	36,400	0.0084	172	49,600	2.64
83	1,700	1,300	93,000	0.0096	473	127,000	2.67
84	1,770	1,350	104,000	0.0087	501	143,000	2.85
116	1,310	1,010	89,000	0.0063	510	151,000	6.40
123	488	373	36,800	0.0047	237	55,500	5.05
126	740	567	80,000	0.0032	415	102,000	3.62
128	360	276	54,000	0.0025	186	71,500	4.35

TABLE 4. SAMPLE RESULTS AT t_0 = 150°F. (Pr_0 = 1.43)

Run	h, B.t.u./(hr.)(°F./sq. ft.)	Nu_0	Re_0	β	Nu_b	Re_b	Pr_b
85	458	380	32,000	0.0112	148	51,500	4.10
89	1,080	897	63,500	0.0143	319	103,500	3.16
93	1,710	1,420	108,000	0.0130	550	175,000	4.05
133	333	276	49,500	0.0052	172	75,000	4.29
137	900	745	117,500	0.0063	453	182,000	4.64
142	432	358	41,000	0.0078	200	75,600	5.85

for all runs except those with inlet or outlet temperatures between 95° and 100°F. This temperature corresponded to the region where the enthalpy was changing most severely and, on the basis of the water results, was due to errors in the enthalpy values rather than in the temperature measurements.

The heat transfer coefficients computed from Equation (1) are tabulated for a few sample runs in Tables 1 to 4 for the four wall temperatures.* Corresponding values of the Nusselt and Reynolds numbers evaluated at both the wall and bulk fluid temperature are also shown. These numbers were obtained by use of the fluid properties given in Figures 5 and 6.

The quantity β shown in the tables is proportional to the heat transfer rate and is useful in applying Deissler's (7) theory of heat transfer with variable physical properties.

The heat transfer coefficients are seen from the tabular values to be large, particularly in Table 2, where the carbon dioxide was closest to the critical point in most runs. The results are plotted as Nu_0 vs. Re_0 in Figures 9 to 12, where the points refer to the experimental results and the lines to theoretical predictions described in the following section.

*Tabular material has been deposited as document 5118 with the American Documentation Institute, Photoduplication Service, Library of Congress, Washingron 25, D.C., and may be obtained for $1.25 for photoprints or 35-mm. microfilm.

PREDICTION OF HEAT TRANSFER COEFFICIENTS

The results were first compared with the dimensionless correlations of the Dittus-Boelter, Sieder and Tate, and Chilton types. In the Dittus-Boelter equation all fluid properties were evaluated at the bulk temperature. The data showed a systematic deviation (as high as 50%) with the heat transfer rate. In the Sieder and Tate equation the properties are all evaluated at the bulk temperature except the viscosity used in the ratio $(\mu_0/\mu_b)^{0.14}$. The agreement was also unsatisfactory, the deviations again being systematic with β and actually somewhat larger than for the Dittus-Boelter relationship. In the Colburn correlation all the properties except c_p are evaluated at a film temperature midway between the bulk and wall values. This approach showed deviations as large as +127 and −74%; in this case they were not systematic with respect to β.

If the temperature and velocity profiles across the tube can be computed, the bulk mean temperature can be evaluated and used in Equation (1) to determine h for comparison with the experimental results. The following equations for the rates of momentum and heat transfer have been used in this way to predict semitheoretical expressions for the heat transfer coefficient.

$$\tau = \frac{\mu\, du}{dy} + \rho\epsilon \frac{du}{dy} \qquad (3)$$

$$q = -k \frac{dt}{dy} - \rho\epsilon_h c_p \frac{dt}{dy} \qquad (4)$$

Most of these developments have been based upon constant fluid properties and therefore are applicable only for the hypothetical case of no heat transfer. Although some of the resulting correlations have been satisfactory for small variations in physical properties, they would not be expected to apply for a fluid in the critical region.

Recently this method of approach has been expanded in an attempt to handle the case of large variations in properties. What is necessary is a fundamental relationship between temperature and property accurate enough to represent the data and still simple enough to allow the solution of Equations (3) and (4). Deissler in a series of papers (*4* to *8*) has proposed a logarithmic relationship for viscosity of the form $\mu/\mu_0 = b(t/t_0)^{\alpha_2}$, where b and α_2 are constant. Assumptions are required in handling Equations (3) and (4) and the set proposed by Deissler is as follows:

The eddy diffusivities for heat and momentum transfer ϵ_h and ϵ are the

same. In the carbon dioxide data reported here, the Reynolds number was always above 30,000 and the Prandtl number greater than unity. Hence the Peclet number ($Pe = Re\ Pr$) exceeded 30,000. Under these conditions this assumption is probably a good one. Fortunately, also, the ratio ϵ_h/ϵ can vary considerably about unity and not significantly affect the computed profiles.

Assumptions are necessary for the variation of eddy diffusivity with distance from the tube wall and many have been suggested by various investigators. Deissler (*6, 8*) proposed the following expressions which were used for this investigation:

$$\epsilon = (n^2)uy\left[1 - \exp\left(-\frac{n^2uy}{\mu/\rho}\right)\right] \quad (5)$$

for flow close to wall;

$$\epsilon = m^2\frac{(du/dy)^3}{(d^2u/dy^2)^2} \quad (6)$$

for flow at a distance from the wall.

$$n = 0.124$$

$$m = 0.36$$

The variation in shear stress τ and heat transfer rate q across the tube has a negligible effect on the velocity and temperature profiles. These quantities do vary with radial position. However, there is evidence to indicate that this variation does not significantly affect the profiles.

With the three assumptions, Equations (3) and (4) may be written in the following dimensionless forms:

$$1 = \left\{\frac{\mu}{\mu_0} + \frac{\rho}{\rho_0}n^2u^*y^* \cdot\left[1 - \exp\left(-\frac{n^2u^*y^*}{(\mu/\mu_0)(\rho_0/\rho)}\right)\right]\right\}\frac{du^*}{dy^*} \quad (7)$$

$$1 = \left\{\frac{k}{k_0Pr_0} + \frac{\rho}{\rho_0}\frac{c_p}{c_{p_0}}n^2u^*y^* \cdot\left[1 - \exp\left(-\frac{n^2u^*y^*}{(\mu/\mu_0)(\rho_0/\rho)}\right)\right]\right\}\frac{dt^*}{dy^*} \quad (8)$$

for flow close to the wall (up to a distance parameter of $y^* = 26$).

Analogous expressions are obtained for flow at a distance from the wall by use of Equation (6).

The dimensionless velocity and distance parameters are defined in the conventional way:

$$u^* = \frac{u}{(\tau_0/\rho_0)^{1/2}} \quad (9)$$

$$y^* = \frac{(\tau_0/\rho_0)^{1/2}}{\mu_0/\rho_0}y \quad (10)$$

The dimensionless temperature has been defined by Deissler as follows:

$$t^* = \frac{(t_0 - t)c_{p_0}\tau_0}{q_0(\tau_0/\rho_0)^{1/2}} = \frac{1}{\beta}\left(1 - \frac{t}{t_0}\right) \quad (11)$$

and so

$$\beta = \frac{q_0(\tau_0/\rho_0)^{1/2}}{c_{p_0}\tau_0t_0} \quad (12)$$

Thus β may be considered a dimensionless heat flux and is directly proportional to the heat transfer rate at the wall.

It is noted in Equations (7) and (8) that the fluid properties occur as ratios to the wall-temperature values. Hence the functional relationship

$$\left(\frac{\mu}{\mu_0}\right) = b\left(\frac{t}{t_0}\right)^{\alpha}$$

and similar ones for specific heat and thermal conductivity are convenient. In applying this approach to the carbon dioxide data, it was necessary to use three different α and b values to cover the required temperature range. At a distance from the critical point the variation of properties with temperature would be more uniform and a single value of α and b might suffice.

Equations (7) and (8) and their counterparts for flow far from the wall were integrated by use of the property data given in Figures 5 and 6. Then bulk means values of temperature and velocity were computed. Finally Nusselt and Reynolds numbers were compiled. The stepwise operations necessary in obtaining the profiles, and their integration to obtain bulk values, necessitate a great number of numerical calculations. Thus the solutions and calculations were programed and carried out on an Electrodata model 30-201 digital computer.

Analysis of the equations shows that the solutions are obtained most conveniently for constant wall temperature and constant value of heat transfer rate or, more precisely, constant value of β. Hence the computations were made for the four wall temperatures studied experimentally and for a series of β values at each wall temperature. The β values were chosen to agree as closely as possible with the experimental range of heat transfer rates. Since it was possible to operate the equipment only at a constant heat transfer rate, q_0, but not β, each experimental point corresponds to a different β. In Figures 9 to 12 the points are identified according to the range of β values to which they correspond.

The computed results are shown in Figures 9 to 12 as solid lines for specific values of β. The variation of the Nusselt number with β on these figures is particularly interesting. In Figure 9 both predicted and experimental results show a decrease in Nu with an increase in β, but the effect is small. Since the fluid temperature is always less than the wall value and the latter is 100°F. for this case, the fluid is not in the region (95° to 105°F.) of most pronounced change in properties with temperature. In Figure 10 the predicted curves show Nu first to increase then decrease as β increases. Examination of the data points out the same trend. This unusual variation is believed to be caused by the fact that now the wall temperature is such that the fluid properties are changing very rapidly, and indeed the specific heat passes through a maximum (Figure 5). Agreement between experimental and predicted results is not so good as in Figure 9 but is still satisfactory.

In Figure 11 for a wall temperature of 130°F. the data show a continuous increase in Nu with β and are in good agreement with the predicted curves for $\beta = 0.004$ and 0.008. The predicted results also show at $\beta = 0.012$ the reverse trend that was found in Figure 10. At this higher wall temperature of 130°F. the bulk fluid temperature would have to be low in order for the temperature profile to pass through the region of maximum change in physical properties. This means that the temperature difference between bulk fluid and wall would be large and lead to a high heat transfer rate. Hence the decrease in Nu with β (at high values of β) predicted in Figure 11 is expected. Experimentally it was not possible to operate at heat transfer rates high enough to reach β values above 0.0096, and so this reverse trend was not observed.

When the wall temperature has risen to 150°F., the fluid temperatures are above the critical range and a continuous increase in Nu with β is observed. The agreement between experimental and predicted results is quite satisfactory.

In summary, two points stand out in Figures 9 to 12. The first is that the solution of the rate of momentum and heat transfer equations proposed by Deissler has correctly predicted the variation in heat transfer coefficient in the critical range. The second is that in the critical region the Nusselt number changes with heat transfer rate or β and that the direction of this change depends upon which side of the critical temperature is involved. Thus in Figure 9, where the temperature was less than the critical value, the Nusselt number decreased with β but in Figure 12, where the temperature was above the critical, the opposite occurred.

It appears from this investigation that the theoretical method is adequate for handling heat transfer problems in the critical region. However, it is too complicated and requires too much time for most applications. Hence there is a need to develop a generalized and simplified substitute for the theoretical approach.

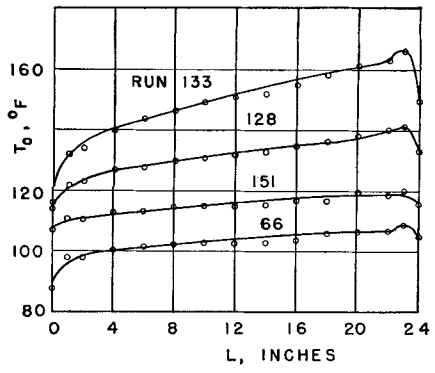

Fig. 8. Wall temperature profiles with flow.

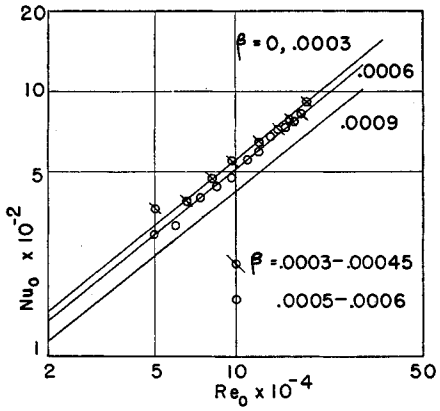

Fig. 9. $Nu_0 = f(Re_0, \beta)$, $T_0 = 100°F.$ experimental and theoretical results.

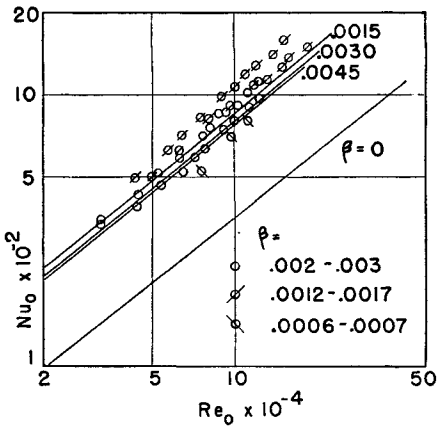

Fig. 10. $Nu_0 = f(Re_0, \beta)$, $T_0 = 110°F.$ experimental and theoretical results.

GENERALIZED CORRELATIONS FOR ESTIMATING HEAT TRANSFER COEFFICIENTS

For the prediction of the Nusselt number from the curves in figures such as 9 to 12, the wall temperature and β must be known. Deissler (*6*) suggested that the effect of β could be eliminated by evaluating Nu and Re at a reference temperature t_x located between the wall and bulk values. In a later paper Deissler (*7*) computed, according to his theory, curves similar to these Figures 9 to 12 for water at 5,000 lb./sq. in. abs., about 1,800 lb./sq. in. abs. above the critical pressure. The reference temperature required to make all the separate curves coincide with the $\beta = 0$ line was then determined. The result was a plot of t_x vs. t_0/t_b with separate curves for each wall temperature. Eckert (*10*) suggested that the effect of t_0 might be eliminated by plotting x [equal to $(t_x - t_b)/(t_0 - t_b)$] vs. $(t_m - t_b)/(t_0 - t_b)$, where t_m is the transposed critical temperature. This latter quantity is the temperature, at a specified pressure, for which the specific heat is a maximum. Figure 13 is such a plot and does indicate that all the data for various wall temperatures is brought together on a single curve. Thus Figure 13 plus the $\beta = 0$ line for a given wall temperature may be used to replace the extensive calculations associated with the prediction method previously described. Additional simplification is obtained from the fact that the wall temperature affects the $\beta = 0$ curves only through the Prandtl number, Pr_0. This follows from the condition that the temperature across the tube is constant at $\beta = 0$, the case of no heat transfer. This constant temperature is the wall temperature and is the one at which the Prandtl number should be evaluated. Since the $\beta = 0$ curves are essentially straight lines on the Nu vs. Re plots, this means that the prediction method can be reduced to Figure 13 and an equation of the form

$$Nu_x = a(Re_x)^b(Pr_0)^c \qquad (13)$$

Finally it may be noted that Figure 13 can be divided approximately into three straight-line sections as shown in Table 5

TABLE 5.

$(t_m - t_b)/(t_0 - t_b)$	x
< 0	0
0 to 1.0	$(t_m - t_b)/(t_0 - t_b)$
> 1.0	1.0

Since $x = (t_x - t_b)/(t_0 - t_b)$, the three sections of the curve suggest the simple rules shown in Table 6 for t_x in terms of the relationship between t_m and t_0 and t_b.

TABLE 6.

$(t_m - t_b)/(t_0 - t_b)$	Reference temperature, t_x
< 0	t_b
0 to 1.0	t_m
> 1.0	t_0

It may be noted that these reference-temperature proposals suggest that when t_0 and t_b are both below the transposed critical value t_m, the reference temperature to use is the wall temperature.

In final form the simplified method consists of Equation (13) and the rules for evaluating the reference temperature shown in Table 6. Using the $\beta = 0$ lines computed by Deissler for water the constants a, b, and c in Equation (13) were numerically evaluated so that the equation takes the form

$$Nu_x = 0.0266(Re_x)^{0.77}(Pr_0)^{0.55} \qquad (14)$$

Equation (14) and Table 6 were first tested by application to the computed points of Deissler for water. The results (Figure 14) show good agreement with Equation (14), an indication that the procedure is satisfactory for supercritical water at 5,000 lb./sq. in. abs. Next the reference temperature rules and Equation (14) were applied to the carbon dioxide data obtained in this study. The comparison, shown in Figure 15, indicates that Equation (14) is about 30% low. The solid line obtained by keeping the

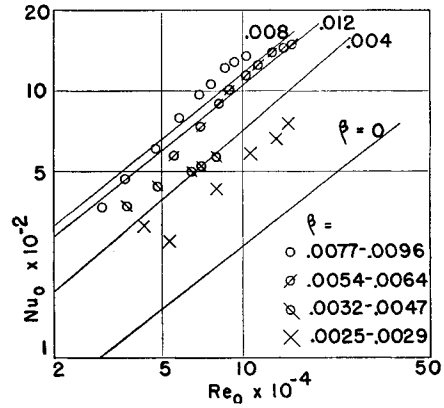

Fig. 11. $Nu_0 = f(Re_0, \beta)$, $T_0 = 130°F.$ experimental and theoretical results.

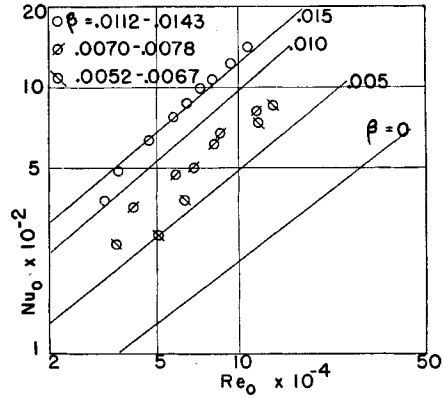

Fig. 12. $Nu_0 = f(Re_0, \beta)$, $T_0 = 150°F.$ experimental and theoretical results.

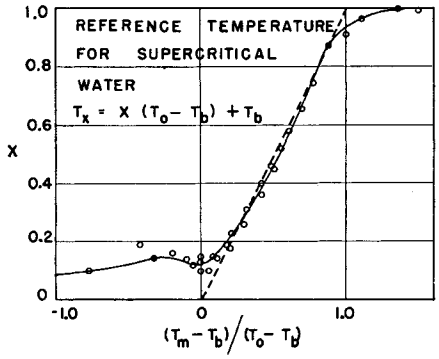

Fig. 13. Reference temperature for supercritical water; $T_x = X(T_0 - T_b) + T_b$.

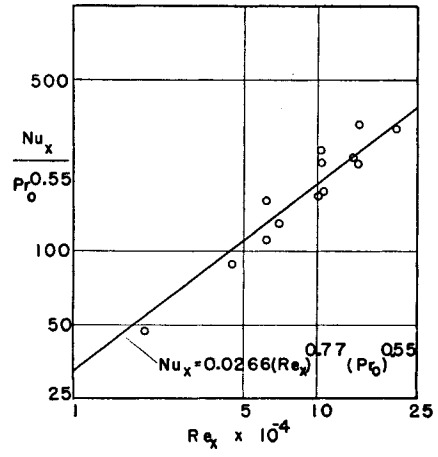

Fig. 14. Supercritical water data after application of reference temperature rule.

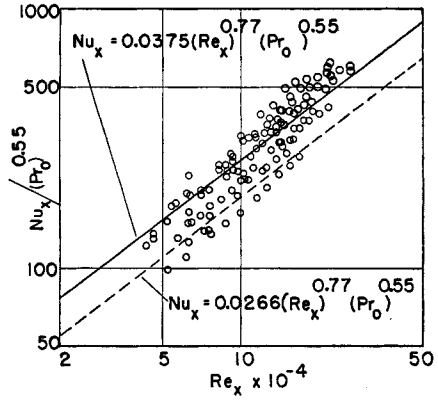

Fig. 15. CO_2 data after application of reference temperature rule.

same exponents on Re_x and Pr_0 but increasing the coefficient fits the data much better, the average deviation being 16%.

Failure of Equation (14) to predict the carbon dioxide data accurately is believed due to inadequacy of the mixture rule in the close proximity of the critical point. Thus the water results are at a reduced pressure of 1.6 and for carbon dioxide the reduced pressure is only 1,200/1,070 = 1.1. While Deissler's theory predicted the experimental results in this region very close to the critical point, the simplified approach based upon the reference temperature rule did not. It is concluded that the simplified approach may be satisfactory as long as the critical point is not approached too closely. More work with carbon dioxide and other fluids is necessary in order to define more definitely the region of applicability of the reference temperature rule.

ACKNOWLEDGMENT

J. W. Smith of the Statistical Department, Purdue University, assisted with the programing of the calculations on the computer. The Engineering Experiment Station and Purdue Research Foundation provided financial assistance.

NOTATION

c_p = specific heat at constant pressure, B.t.u./(lb.)(°F.)
h = local coefficient of heat transfer between fluid and tube wall, B.t.u./(hr.)(sq. ft./°F.)
H = enthalpy of carbon dioxide, B.t.u./lb.
H_1 = enthalpy at entrance to test section
I = Electric current
k = thermal conductivity, B.t.u./(hr.)(ft./°F.)
L = length of test section, ft.
Nu = Nusselt number, dimensionless
Pe = Peclet number ($Pe = Pr\ Re$), dimensionless
Pr = Prandtl number, dimensionless
q = heat transfer rate per unit area. q_0 = heat transfer rate per unit area at the tube wall, B.t.u./(hr.)(sq. ft.)
R_t = total electrical resistance of test section, ohms
Re = Reynolds number, dimensionless
t = temperature, °F.
t^* = dimensionless temperature defined by Equation (11)
u = point velocity in direction of flow, ft./hr.
u^* = dimensionless velocity defined by Equation (9)
w = weight rate of flow of carbon dioxide in tube, lb./hr.
z = distance from end of test section, measured in direction of flow, ft.
y = radial distance in tube, measured from tube wall, ft.
y^* = dimensionless distance defined by Equation (10)
β = dimensionless parameter proportional to heat transfer rate, defined by Equation (12)
ϵ = eddy diffusivity, sq. ft./hr.
ϵ_h = eddy diffusivity for heat transfer, sq. ft./hr.
μ = viscosity of fluid, lb./(hr. ft.)
ρ = density of fluid, lb./cu. ft.
τ = shear stress per unit area, poundals/(sq. ft.)

Subscripts

0 = wall conditions
b = bulk mean conditions of fluid

LITERATURE CITED

1. Boelter, L. M. K., R. C. Martinelli, and F. Jonassen, *Trans. Am. Soc. Mech. Engrs.*, **63**, 447 (1941).
2. Colburn, A. P., *Trans. Am. Inst. Chem. Engrs.*, **29**, 174 (1933).
3. Comings, E. W., and R. S. Egly, *Ind. Eng. Chem.*, **33**, 1224 (1941).
4. Deissler, R. G., *Natl. Advisory Comm. Aeronaut. Tech. Note* 2138 (1950).
5. ———, *Natl. Advisory Comm. Auronaut. Rept.* E52F05 (1952).
6. ——— and C. S. Eian, *Natl. Advisory Comm. Aeronaut. Tech. Note* 2629 (1952).
7. Deissler, R. G., and M. F. Taylor, *Natl. Advisory Comm. Aeronaut. Rept.* E53B17 (1953).
8. ———, *Natl. Advisory Comm. Aeronaut. Tech. Note* 3145 (1954).

8A. Deissler, R. G., *Trans. Am. Soc. Mech. Engrs.*, **76**, 73 (1954).

9. Dittus, F. W., and L. M. K. Boelter, *Univ. Calif. (Berkeley), Publ. Eng.*, **2**, 443 (1930).
10. Eckert, E. R. G., Discussion, *Trans. Amer. Soc. Mech. Engrs.*, **76**, 83 (1954).
11. Franck, E. U., *Chem.-Eng.-Techn.*, **25**, 238 (1953).
12. Kiyama, R., and T. Makita, *Rev. Phys. Chem., Japan*, **22**, 49 (1952).
13. Krausshold, H., *Forsch. Gebeite Ingenieurw.*, **5B**, 186 (1934).
14. Lenoir, J. M., and E. W. Comings, *Chem. Eng. Progr.*, **47**, 223 (1951).
15. Michels, A., and C. Michels, *Proc. Roy. Soc. (London)*, **A153**, 201 (1935).
16. Michels, A., and S. R. de Groot, *Appl. Sci. Research*, **A1**, 94 (1948).
17. Naldrett, S. N., and O. Maass, *Can. J. Research*, **18B**, 322 (1940).
18. Phillips, P., *Proc. Roy. Soc. (London)*, **87**, 48 (1912).
19. Plank, R., and J. Kuprianoff, *Z. ges. Kälte-Ind.*, **36**, 41 (1929).
20. Prandtl, L., *Physik. Z.*, **11**, 1072 (1910).
21. Reynolds, Osborne, *Proc. Manchester Lit. Phil. Soc.*, **14**, 7 (1874).
22. Schroer, E., and G. Becker, *Z. physik. Chem.*, **173A**, 178 (1935).
23. Sellschopp, W., *Forsch. Gebeite Ingenieurw.*, **5B**, 162 (1934).
24. Sieder, E. N., and G. E. Tate, *Ind. Eng. Chem.*, **28**, 1429 (1936).
25. Stakelbeck, H., *Z. ges. Kälte-Ind.*, **40**, 33 (1933).
26. Stoljarow, E. A., *J. physik. Chem. (U.S.S.R.)*, **24**, 166 (1950).
27. Von Karman, T., *Trans. Am. Soc. Mech. Engrs.*, **61**, 705 (1939).
28. Zerby, C. D., "O.R.N.L. Pump Brochure," Oak Ridge Nat. Lab. (1954).